

Anisotropy in homogeneous dislocation nucleation by nanoindentation of single crystal Cu

X.H. Liu,^a J.F. Gu,^{a,*} Y. Shen^a and C.F. Chen^{b,*}

^aShanghai Key Laboratory of Materials Laser Processing and Modification, School of Materials Science and Engineering, Shanghai Jiao Tong University, Shanghai 200240, China

^bDepartment of Physics and High Pressure Science and Engineering Center, University of Nevada, Las Vegas, NV 89154, USA

Received 29 September 2007; accepted 12 November 2007

Available online 20 December 2007

This paper addresses the anisotropy in homogeneous dislocation nucleation by nanoindentation on different crystallographic surfaces in perfect single crystal Cu. The interatomic potential finite-element model is used to extend the computational cell size to micron-scale for eliminating boundary effects. Simulation results reveal that significant anisotropy exists for the critical indentation depth, the critical resolved shear stress and the critical indentation hardness. The calculated indentation moduli for the (001), (011), (111) surfaces fit the experimental data well.

© 2007 Acta Materialia Inc. Published by Elsevier Ltd. All rights reserved.

Keywords: Anisotropy; Nanoindentation; Dislocation nucleation

Anisotropy of single crystals has received considerable interest, motivated by the development of experimental instruments and numerical approaches in the past few years. On the experimental front, nanoindentation has been widely used to investigate the mechanical properties of different crystallographic surfaces of single crystals [1–4]. On the numerical side, atomistic simulations have also been performed to characterize the anisotropy. For instance, Diao et al. [5] showed the yield strength difference in Au nanowires between the [100] and [111] orientations. Tsuru and Shibutani [6] performed simulations of nanoindentation on three different surfaces in Al and Cu to probe the anisotropic effects in the elastic and incipient yield event. Tschopp and McDowell [7] addressed the dependence of homogeneous dislocation nucleation on the crystallographic orientation of Cu under uniaxial tension and compression. Unlike the experimental investigations on macro-scale blocks, these numerical studies focused mainly on nano-scale systems, which inevitably include boundary effects due to their small size. To probe the anisotropy of mechanical properties without such boundary effects, it is highly desirable to extend the size of the investigated

system. The interatomic potential finite-element model (IPFEM) proposed by Li et al. [8–10] affords an accurate and efficient method for dealing with large-length-scale systems and has been validated by a comparison of indentation results with molecular dynamics (MD) simulations [8,10]. This paper reports on an investigation into the anisotropy in nanoindentation-induced homogeneous dislocation nucleation in perfect single crystal Cu with large-length-scale simulations by IPFEM, which provides insights into the anisotropy in mechanical behavior and expands the scope of understanding of these fundamental mechanical properties.

A cylinder of single crystal Cu aligned along the x_2 direction is specially designed to be indented on its top surface. Compared with block models used in some nanoindentation simulations [6,8–10], the choice of the cylinder can further reduce the boundary effects on indentation behavior, as the indentation deformation is nearly axisymmetric. The radius and height of the cylinder are set to 1 μm and 5 μm , respectively, as the lateral boundaries should be taken at least ~ 50 times the maximum contact length (< 200 Å in the present simulations) away from the indented area, and the height should be taken as more than five times the radius so as to eliminate the effects of the lateral and bottom boundaries [11]. It is extremely arduous to simulate such a large model containing more than 1000 billion Cu atoms for atomistic simulation methods but suitable

* Corresponding authors. Tel.: +86 21 34203743; fax: +86 21 34203742; e-mail addresses: gujf@sjtu.edu.cn; chen@physics.unlv.edu

for IPFEM. The top and lateral surfaces of the cylinder are traction-free and the bottom is fixed. An analytic rigid spherical indenter is used to indent on the cylinder along the central axis, and its radius is set to 500 Å, the approximate tip radius of a nominally sharp Berkovich indenter in nanoindentation experiments [12]. The contact between the indenter and the top surface of the cylinder is frictionless. The embedded-atom method potential for Cu proposed by Mishin et al. [13] is employed to model the constitutive relation for its accurate description of finite shear deformation compared with the *ab initio* density functional theory calculation [10], which is important for predicting dislocation nucleation accurately.

The IPFEM simulations are performed as quasi-static analysis at a temperature of absolute 0 K with ABAQUS/Standard software [14]. In each indentation step, the deformation gradient for each integration point is calculated based on the updated displacement field, and then the positions for the neighboring atoms are updated according to the Cauchy–Born hypothesis [15]. The Cauchy stress σ and tangent modulus C at the current configuration are obtained based on the interatomic potential within the framework of hyperelasticity [10,15,16]. The onset of local instability of the crystal lattice occurs as $\Lambda(\mathbf{k}, \mathbf{w}) = (C_{ijkl}w_iw_jk_k + \sigma_{ji})k_jk_l \leq 0$, where \mathbf{k} and \mathbf{w} are normalized vectors which are defined as the wave vector and the polarization vector, respectively [8]. Once the minimum $\Lambda(\Lambda_{\min})$ becomes non-positive and the corresponding vectors \mathbf{k} and \mathbf{w} are orthogonal to each other, the point of instability may be identified with dislocation nucleation, and the two vectors correspond to the slip plane and slip direction, respectively. For simplicity, vectors \mathbf{k} and \mathbf{w} are explicitly traced to obtain the Λ_{\min} at each integration point within the 24 known slip systems of an fcc crystal, the $\langle 110 \rangle$ and $\langle 112 \rangle$ slip directions on $\{111\}$ slip planes.

IPFEM's capability to eliminate boundary effects has been demonstrated in the calculations (not shown). It yields almost the same results as those of MD in nano-scale. But asymptotic results have been observed on increasing the system sizes, with significant difference between the saturated values of mechanical properties and those for nano-scale, indicating both the elimination and existence of boundary effects in micron- and nano-scales, respectively.

To investigate the anisotropy, extensive simulations have been performed on different indentation surfaces, with the cylinder aligned along 37 orientations distributed almost uniformly in the stereographic triangle (Fig. 1). In all cases, the calculations are terminated at the onset of the first dislocation nucleation predicted by the Λ criterion. As an example, the simulation results of indentation on the (111) surface are shown in Figure 2. Three gray elements positioned symmetrically around the central axis of the cylinder beneath the top surface of (111) are predicted as the dislocation nucleation sites. The elements are colored according to the Λ_{\min} values, and the gray elements indicate that their Λ_{\min} values are non-positive. At each nucleation site, two Shockley partial dislocations are equally likely to be activated, and the corresponding slip systems are denoted in Figure 2b. The results differ from those of Zhu et al. [10]

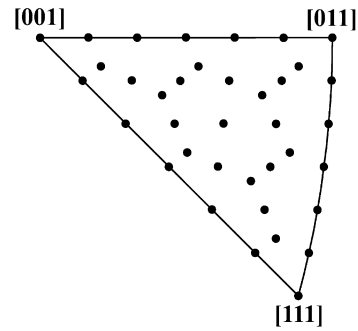


Figure 1. The inverse pole figure showing the 37 axis orientations of the cylinder.

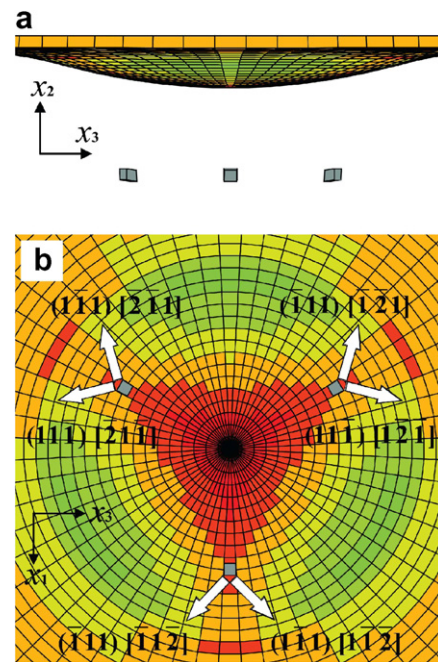


Figure 2. (a) Side and (b) bottom views of the first three homogeneous dislocation nucleation sites beneath the (111) surface. The predicted slip systems are denoted in (b). In both cases, $x_1 = [11\bar{2}]$, $x_2 = [111]$, $x_3 = [1\bar{1}0]$.

in which Shockley partial dislocations identified on the three $\{111\}$ -type slip planes nucleated asynchronously owing to the loss of the threefold symmetry of lateral boundaries in the block model used.

The critical indentation depths required for homogeneous dislocation nucleation predicted by the Λ criterion for all 37 cases are recorded, and the contour within the stereographic triangle is obtained through linear interpolation (Fig. 3a). It is obvious that significant anisotropy of the critical indentation depth exists in single crystal Cu. The (111) surface requires the largest indentation depth for dislocation nucleation, while the (001) surface requires the lowest, which is nearly one-third of the former.

The character of the first homogeneous dislocation is Shockley partial dislocation for all indentation surfaces, and the critical resolved shear stress (CRSS) is then calculated on respective slip system for all cases and interpolated to obtain its distribution (Fig. 3b). The CRSS

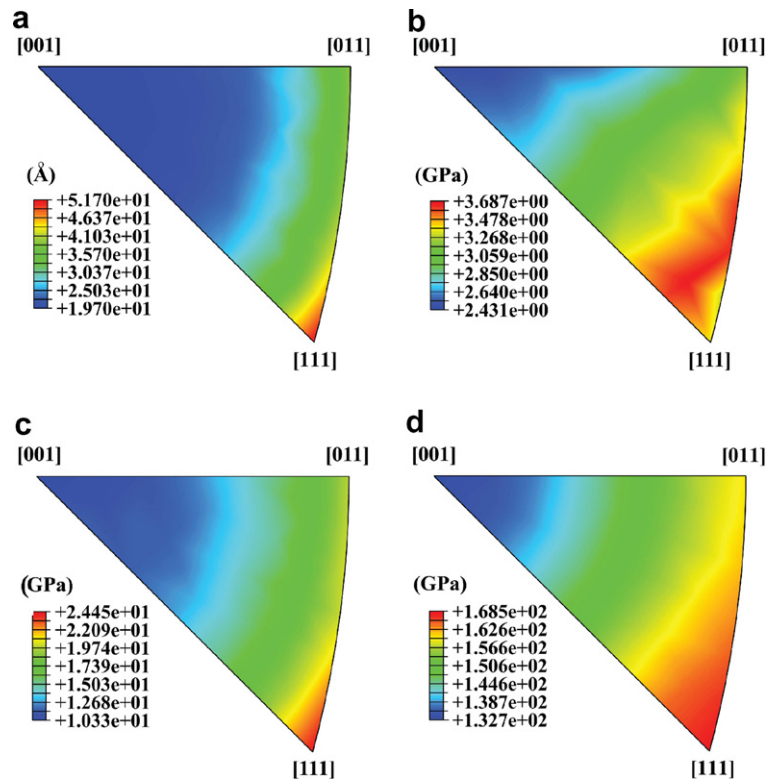


Figure 3. (a) Critical indentation depth, (b) CRSS, (c) critical indentation hardness and (d) indentation modulus as functions of the indentation surface.

varies with the indentation surface instead of being a constant as a result of its dependence on the local stress state at the nucleation site. Thus, CRSS cannot serve as a criterion to predict homogeneous dislocation nucleation, which is in accordance with the view of previous studies [10,17,18]. It is worth noting that the minimum CRSS of 2.43 GPa is larger than the ideal shear strength of 2.16 GPa by Ogata et al. [19], which can be attributed to the nanoindentation-induced large triaxial stress at the site of the first dislocation nucleation.

As the indentation hardness H of a material is equivalent to the mean pressure P under the indenter, typically defined as $H = P = L/A$, where L and A are the load and the contact area, respectively, the corresponding critical indentation hardness H_c and critical mean pressure P_c can be calculated at the first dislocation nucleation. The calculations show that, if the radius of the spherical indenter and the size of the cylinder are large enough without introducing boundary effects, the first dislocation always nucleates within the material, and H_c (P_c) is constant for a certain indentation surface, regardless of the indenter radius, owing to the similar geometries of indents at the onset of the first dislocation nucleation. As noted in Refs. [6] and [20], the critical mean pressure is one of the most important indicators of dislocation nucleation. It is further inferred that H_c (P_c) can be an intrinsic property of single crystal Cu, and it locates the transition point from an elastic regime to a plastic one in the whole indentation hardness profile. It can be seen from Figure 3c that H_c (P_c) exhibits a high degree of anisotropy similar to that of the critical indentation depth. The (111) and (001) surfaces are the

hardest and softest surfaces with the critical indentation hardness of 24.5 GPa and 10.3 GPa, respectively, which are dramatically higher than the measured hardness in nanoindentation experiments by Wang et al. [4] owing to the absence of plastic deformation.

The indentation modulus is an important parameter in nanoindentation and can be obtained based on the Hertzian elastic theory [21]. The relation between the load L and indentation depth h in the elastic regime can be described as $L = (4/3)E_r R^{1/2} h^{3/2}$, where R is the radius of the spherical indenter, and E_r is the reduced modulus. While E_r is given by $1/E_r = 1/E + (1 - \nu_i^2)/E_i$, where E_i and ν_i are Young's modulus and Poisson's ratio of the indenter, and E is the indentation modulus of the material [1]. In the present study, the indenter is ideally rigid, so E is equal to E_r , which can be obtained by fitting the elastic part of the P - h curve to the Hertzian solution. The contour of E is shown in Figure 3d. On the whole, E values for the (001), (011), (111) surfaces agree well with the experimental data [4], while the small deviation from the respective experimental average value may be due to the assumption of the lower temperature of 0 K, the rigid indenter and the frictionless contact between the indenter and the top surface in this work. The difference in E values between the (001) and (111) surfaces reaches $\sim 20\%$, exhibiting the anisotropy in single crystal Cu.

In summary, the anisotropy in nanoindentation-induced homogeneous dislocation nucleation in perfect single crystal Cu has been investigated based on the large-length-scale simulations by IPFEM, which is capable of eliminating boundary effects. The critical

indentation depth shows a high degree of anisotropy. The CRSS varies with the indentation surface and depends on the local stress state at the nucleation site. The critical indentation hardness, defined the same as the critical mean pressure, can be referred as an intrinsic material constant and also exhibits significant anisotropy. The indentation moduli for the (001), (011), (111) surfaces agree well with the experimental data and have a 20% degree of anisotropy.

This work is supported by DOE under the Cooperative Agreement DE-FC52-06NA26274 at UNLV. J.F. Gu and Y. Shen are also supported by the National Natural Science Foundation of China under Grant No. 50601017 and 50601018, respectively.

- [1] J.J. Vlassak, W.D. Nix, *J. Mech. Phys. Solids* 42 (1994) 1223.
- [2] J.D. Kiely, J.E. Houston, *Phys. Rev. B* 57 (1998) 12588.
- [3] W. Wang, K. Lu, *J. Mater. Res.* 17 (2002) 2314.
- [4] W. Wang, K. Lu, *Philos. Mag. A* 86 (2006) 5309.
- [5] J. Diao, K. Gall, M.L. Dunn, *Nano Lett.* 4 (2004) 1863.
- [6] T. Tsuru, Y. Shibutani, *Phys. Rev. B* 75 (2007) 035415.
- [7] M.A. Tschopp, D.L. McDowell, *Appl. Phys. Lett.* 90 (2007) 121916.
- [8] J. Li, K.J. Van Vliet, T. Zhu, S. Yip, S. Suresh, *Nature* 418 (2002) 307.
- [9] K.J. Van Vliet, J. Li, T. Zhu, S. Yip, S. Suresh, *Phys. Rev. B* 67 (2003) 104105.
- [10] T. Zhu, J. Li, K.J. Van Vliet, S. Ogata, S. Yip, S. Suresh, *J. Mech. Phys. Solids* 52 (2004) 691.
- [11] A.E. Giannakopoulos, P.L. Larsson, R. Vestergaard, *Int. J. Solid. Struct.* 31 (1994) 2679.
- [12] A. Gouldstone, H.J. Koh, K.Y. Zeng, A.E. Giannakopoulos, S. Suresh, *Acta Mater.* 48 (2000) 2277.
- [13] Y. Mishin, M.J. Mehl, D.A. Papaconstantopoulos, A.F. Voter, J.D. Kress, *Phys. Rev. B* 63 (2001) 224106.
- [14] H.D. Hibbitt, G.I. Karlsson, E.P. Sorensen, *ABAQUS, Reference Manuals V6.5*, 2004.
- [15] J.L. Ericksen, *Phase Transformations, Material Instabilities in Solids*, Academic Press, New York, 1984.
- [16] E. Tadmor, M. Ortiz, R. Phillips, *Philos. Mag. A* 73 (1996) 1529.
- [17] C.L. Kelchner, S.J. Plimpton, J.C. Hamilton, *Phys. Rev. B* 58 (1998) 11085.
- [18] R.E. Miller, A. Acharya, *J. Mech. Phys. Solids* 52 (2004) 1507.
- [19] S. Ogata, J. Li, S. Yip, *Science* 298 (2002) 807.
- [20] T. Tsuru, Y. Shibutani, *Modell. Simul. Mater. Sci. Eng.* 14 (2006) S55.
- [21] K.L. Johnson, *Contact Mechanics*, Cambridge University Press, Cambridge, UK, 2003.